Journal of Applied Fluid Mechanics, Vol. 9, No. 3, pp. 1437-1445, 2016.
Available online at www.jafmonline.net, ISSN 1735-3572, EISSN 1735-3645.
DOI: 10.18869/acadpub.jafm.68.228.24172

Flow and Heat Transfer over an Unsteady Stretching Sheet in a Micropolar Fluid with Convective Boundary Condition

S. A. Shehzad[1†], M. Waqas[2], A. Alsaedi[3] and T. Hayat[2,3]

[1]*Department of Mathematics, Comsats Institute of Information Technology, Sahiwal 57000, Pakistan*
[2]*Department of Mathematics, Quaid-i-Azam University 45320, Islamabad 44000, Pakistan*
[3]*Department of Mathematics, Faculty of Science, King Abdulaziz University, Jeddah 21589, Saudi Arabia*

†Corresponding Author Email: ali_qau70@yahoo.com

(Received October 29, 2014; accepted July 4, 2015)

ABSTRACT

This article is concerned with the flow of micropolar fluid over an unsteady stretching surface with convective boundary condition. The governing partial differential equations are first converted into ordinary differential equations using appropriate transformations and then solved for the series solutions. Influence of micropolar parameter, unsteadiness parameter, boundary parameter, Prandtl number and Biot number on the flow and heat transfer characteristics is examined. Numerical values of local Nusselt number and skin friction coefficient are presented and analyzed. It is observed that temperature is an increasing function of Biot number.

Keywords: Heat transfer**;** Unsteady stretching surface**;** Micropolar fluid; Convective boundary condition.

NOMENCLATURE

Cf_x	skin friction coefficient	Re_x	Reynolds number
f	dimensionless velocity	S	unsteadiness parameter
j	microinertia	T	temperature
h	heat transfer coefficient	T_∞	ambient fluid temperature
g	dimensional microrotation velocity	T_f	hot fluid temperature
k_1	thermal conductivity	u, v	velocity components
k	vortex viscosity	γ	Biot number
K	micropolar parameter	γ^*	spin gradient viscosity
m_0	boundary parameter		
N^*	angular velocity	α	thermal diffusivity
Nu_x	local Nusselt number	ρ	fluid density
Pr	Prandtl number	μ	dynamic viscosity
q_w	surface heat flux		

1. INTRODUCTION

The dynamics of micropolar fluids has been attracted by the recent workers during the last few decades because traditional Newtonian fluids cannot precisely describe the characteristics of fluid flow with suspended particles. Eringen (1966) developed the theory that the local effects arising from the microstructure and the intrinsic motion of the fluid elements should be taken into account. The theory is expected to provide a mathematical model for fluid behavior observed in certain man-made liquids such as polymers, lubricants, fluids with additives, paints, animal blood, colloidal and suspension solutions, etc. The presence of dust or smoke, particularly in a gas may also be modeled

using micropolar fluid model. Consideration of micropolar fluid also has much importance in soldification of liquid crystal. Later Eringen (1972) extended the theory of thermo-micropolar fluids and derived the constitutive laws for fluids with microstructures. The rigid particles in a small volume element rotate about the centroid of the volume element in micropolar fluids. The pioneering work of Eringen (1966) was extended in boundary layer theory by Peddieson and McNitt (1970). Nazar *et al*. (2004) carried out a study to address the stagnation point flow of micropolar fluid over a linearly stretching surface. Ishak *et al*. (2008) reported heat transfer over a stretching surface with variable heat flux in micropolar fluid. Mixed convection flow of micropolar fluid over a nonlinear stretching surface has been discussed by Hayat *et al*. (2008). Stagnation point flow of micropolar fluid towards a vertical permeable surface is examined by Ishak *et al*. (2008). Series solutions for boundary layer flow of micropolar fluid in porous channel were presented by Sajid *et al*. (2009). Yacob *et al*. (2011) investigated melting heat transfer in boundary layer stagnation point flow towards a stretching/shrinking sheet in a micropolar fluid. Rashidi *et al*. (2010) studied the flow of micropolar fluid in a porous channel using differential transform method. Steady flow of a micropolar fluid driven by injection or suction between a porous and non-porous disks is addressed by Motsa *et al*. (2010). Micropolar fluid flow over a shrinking sheet is presented by Yacob *et al*. (2012). Hayat *et al*. (2011a) investigated the boundary layer flow of micropolar fluid with mixed convection and chemical reaction. Ishak *et al*. (2010) explored stagnation point flow of micropolar fluid over a shrinking sheet. Unsteady flow of micropolar fluid over a stretching surface with heat transfer was numerically investigated by Bachok *et al*. (2011).

The flows over a stretching surface with heat transfer has received much attention in the past due to their potential applications in many industrial processes, for example, in continuous casting, glass-fiber production, paper production, metal extrusion, hot rolling, wire drawing, drawing of plastic films, metal and polymer extrusion and metal spinning. Specially, aerodynamic extrusion of plastic sheets is very important operation in polymer industry. This process involves the heat transfer between the surface and the surrounding fluid. The melt issue from a slit is subsequently stretched to obtain the desired quality during the manufacturer of the sheet. Heat transfer in such process has important role in controlling the cooling rate. Interesting studies in this direction may be mentioned by Devi *et al*. (1991), Andersson *et al*. (2000), Nazar *et al*. (2004), Ishak *et al*. (2009), Hayat *et al*. (2012a), Makinde (2012), Shehzad *et al*. (2013a, 2013b) etc. In all these studies heat transfer is discussed either through the prescribed temperature or heat flux at the surface. Recently the more general concept of heat transfer in terms of convective condition has been proposed. The relevant information in this direction is very scrace. For instance Makinde (2010) investigated the heat and mass transfer effects in the steady flow of viscous fluid over a moving vertical plate with convective thermal condition. Makinde and Aziz (2010) discussed the buoyancy driven flow in a porous medium with convective heating. Boundary layer flow of non-Newtonian fluid over a stretching sheet with convective boundary condition was examined by Hayat *et al*. (2011b). Hayat *et al*. (2012b) reported series solutions for mixed convection flow of Casson fluid over a linearly stretching surface in the presence of convective condition. Shehzad *et al*. (2013c) discussed the boundary layer flow of Jeffrey fluid with convective boundary condition in presence of heat and mass transfer near a stagnation point. It can be noted that no attempt is yet presented for unsteady flow subject to convective condition of heat transfer. Hence the present investigation looks at the unsteady flow caused by a stretching sheet with convective condition of heat transfer. Constitutive equations for micropolar fluid are taken into account. Transformation procedure is employed to reduce the partial differential equations into the ordinary differential equations. Series solutions are obtained using a powerful technique namely the homotopy analysis method (HAM) proposed by Liao (2003). This method has been already successfully applied recently for many other interesting problems (Abbasbandy and Shivanian (2011), Hayat *et al*. (2012c, 2012d), Rashidi and Erfani (2012), Rashidi *et al*. (2012), and Shehzad *et al*. (2015)). Convergence of the obtained series solutions is verified. Graphical results are presented and analyzed.

2. MATHEMATICAL MODEL

We consider two-dimensional time-dependent flow of an incompressible micropolar fluid over a stretching sheet. At time $t = 0$, the sheet is impulsively stretched with velocity $U_w(x,t)$ along the x-axis, keeping the origin fixed in the fluid of ambient temperature T_∞. The stationary Cartesian coordinate system has its origin located at the leading edge of the sheet with the positive x-axis extending along the sheet, while the y-axis is measured normal to the surface of the sheet. The governing flow and energy equations are (Bachok *et al*. 2011):

$$\frac{\partial u}{\partial x}+\frac{\partial v}{\partial y}=0, \tag{1}$$

$$\begin{aligned}&\frac{\partial u}{\partial t}+u\frac{\partial u}{\partial x}+v\frac{\partial u}{\partial y}\\&=\left(\frac{\mu+k}{\rho}\right)\frac{\partial^2 u}{\partial y^2}+\frac{k}{\rho}\frac{\partial N^*}{\partial y},\end{aligned} \tag{2}$$

$$\begin{aligned}&\rho j\left(\frac{\partial N^*}{\partial t}+u\frac{\partial N^*}{\partial x}+v\frac{\partial N^*}{\partial y}\right)\\&=\gamma^*\frac{\partial^2 N^*}{\partial y^2}-k\left(2N^*+\frac{\partial u}{\partial y}\right),\end{aligned} \tag{3}$$

$$\frac{\partial T}{\partial t}+u\frac{\partial T}{\partial x}+v\frac{\partial T}{\partial y}=\alpha\frac{\partial^2 T}{\partial y^2} \tag{4}$$

with the boundary conditions

$$\begin{aligned} &u=U_w,\ v=0,\ N^*=-m_0\frac{\partial u}{\partial y},\\ &-k_1\frac{\partial T}{\partial y}=h(T_f-T_\infty)\ \text{at}\ y=0,\\ &u\to 0,\ N^*\to 0,\ ,\ T\to T_\infty\ \text{as}\ y\to\infty. \end{aligned} \tag{5}$$

In the above expressions, u and v are the velocity components in the x and y directions respectively, μ is the dynamic viscosity, ρ is the fluid density, ν is the kinematic viscosity, α is the thermal diffusivity, N^* is the microrotation or angular velocity, T is the fluid temperature, k_1 is the thermal conductivity, h is the convective heat transfer coefficient, $j=\nu/c$ is microinertia, γ^* is the spin gradient viscosity and k is the vortex viscosity. Here for $k=0$, we have the case of viscous fluid. Furthermore, the boundary parameter m_0 has a range $0\le m_0\le 1$. It should be notedthat when $m_0=0$ $\left(\text{called strong concentration}\right)$ then $N^*=0$ near the wall. This represents the concentrated particle flows in which the microelements close to the wall surface are unable to rotate. The case $m_0=1/2$ corresponds to the vanishing of antisymmetric part of the stress tensor and it shows weak concentration of microelements. It is assumed that the stretching velocity $U_w(x,t)$ and the surface heat flux $q_w(x,t)$ are

$$U_w(x,t)=\frac{ax}{1-ct},\ q_w(x,t)=\frac{bx}{1-ct} \tag{6}$$

where a, b and c are rate constants with $a>0$, $b\ge 0$ and $c\ge 0$ (with $ct<1$). The particular forms of $U_w(x,t)$ and $q_w(x,t)$ have been chosen in order to be able to devise a new relation which transform the governing partial differential equations (1) to (4) into a set of ordinary differential equations, thereby facilitating the exploration of the effects of the controlling parameters. The spin-gradient viscosity γ^* can be defined as

$$\gamma^*=\left(\mu+\frac{k}{2}\right)j, \tag{7}$$

where the material parameter (or micropolar parameter) $K=\frac{k}{\mu}$ is the dimensionless viscosity ratio.

The continuity equation (1) is satisfied by introducing a stream function ψ such that $u=\frac{\partial\psi}{\partial y}$ and $v=-\frac{\partial\psi}{\partial x}$. We define the following new variables

$$\begin{aligned} &\eta=\left(\frac{U_w}{\nu x}\right)^{1/2}y,\ \psi=(\nu x U_w)^{1/2}f(\eta),\\ &N^*=U_w\left(\frac{U_w}{\nu x}\right)^{1/2}g(\eta),\ \theta(\eta)=\frac{T-T_\infty}{T_f-T_\infty}. \end{aligned} \tag{8}$$

Now Eqs. (2)-(5) are reduced as

$$(1+K)f'''+ff''-f'^2+Kg'-S\left(f'+\frac{1}{2}\eta f''\right)=0, \tag{9}$$

$$\left(1+\frac{K}{2}\right)g''+fg'-f'g-K(2g+f'')-S\left(\frac{3}{2}g+\frac{1}{2}\eta g'\right)=0, \tag{10}$$

$$\theta''+\Pr(f\theta'-f'\theta)-S\Pr\left(\theta+\frac{1}{2}\eta\theta'\right)=0, \tag{11}$$

$$\begin{aligned} &f(0)=0,\ f'(0)=1,\ g(0)=-m_0 f''(0),\\ &\theta'(0)=-\gamma(1-\theta(0)),\\ &f'(\eta)\to 0,\ g(\eta)\to 0,\ \theta(\eta)\to 0\ \text{as}\ \eta\to\infty, \end{aligned} \tag{12}$$

where primes denote differentiation with respect to η, $\Pr=\nu/\alpha$ is the Prandtl number, $S=c/a$ is the unsteadiness parameter and $\gamma=-h/k_1\left(\frac{\nu x}{U_w}\right)^{1/2}$ is the Biot number.

The skin friction coefficients Cf_x and local Nusselt number Nu_x with heat transfer q_w are given by

$$\begin{aligned} &Cf_x=\left((\mu+k)\frac{\partial u}{\partial y}+kN^*\right)_{y=0},\\ &Nu_x=\frac{xq_w}{k(T_f-T_\infty)},\ q_w=-k_1\left(\frac{\partial T}{\partial y}\right)_{y=0}, \end{aligned} \tag{13}$$

The local Nusselt number and skin friction coefficient in dimensionless forms becomes

$$\begin{aligned} &Nu\,\mathrm{Re}_x^{-1/2}=-\theta'(0),\\ &\mathrm{Re}_x^{1/2}\,Cf_x=(1+(1-m_0)K)f''(0), \end{aligned}$$

where $\mathrm{Re}_x=ax^2/\nu$ is the local Reynolds number.

3. CONVERGENCE OF THE HOMOTOPY SOLUTIONS

It is well known that the series solutions involve the non-zero auxiliary parameters $\hbar_f$, $\hbar_g$ and $\hbar_\theta$. Such parameters are useful in adjusting and controlling the convergence of the HAM solutions. Hence for the range of admissible values of $\hbar_f$, $\hbar_g$ and $\hbar_\theta$, we display the $\hbar$-curves of the functions $f''(0)$, $g'(0)$ and $\theta'(0)$ for 20th-order of approximations. Here Figs. 1-3 show that the range of admissible values of $\hbar_f$, $\hbar_g$ and $\hbar_\theta$ are

$-1.35 \le \hbar_f \le -0.2$, $-1.45 \le \hbar_g \le -0.25$ and $-1.45 \le \hbar_\theta \le -0.30$. The definitions of square residual errors are:

$$\Delta_m^f = \int_0^1 \left[R_m^f(\eta, \hbar_f)\right] d\eta$$

$$\Delta_m^g = \int_0^1 \left[R_m^g(\eta, \hbar_g)\right] d\eta$$

$$\Delta_m^\theta = \int_0^1 \left[R_m^f(\eta, \hbar_\theta)\right] d\eta$$

Figure 4: (a) describes the lowest possible error of f for $\hbar_f \in [-1.30, -0.90]$. Fig. 4: (b) shows the lowest possible error of g for $\hbar_g \in$ [-1.30, -0.85]. Fig. 4(c) describes the lowest possible error of θ for $\hbar_\theta \in [-1.05, -0.95]$. Here Fig. 4 is plotted to ensure the convergence of the quantities in the Figs. 1 – 3.

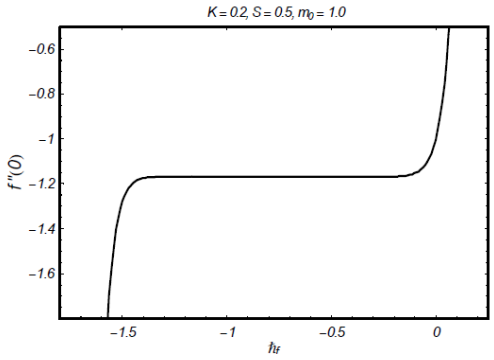

Fig. 1. $\hbar$ -curve for the function *f*.

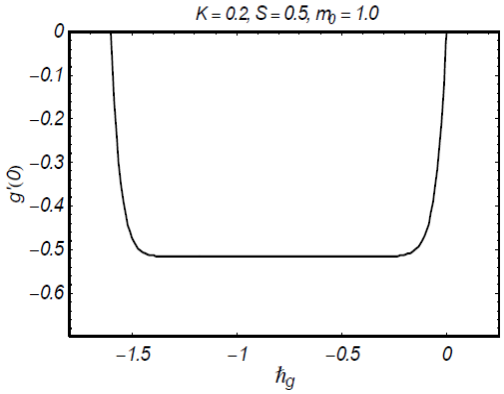

Fig. 2. $\hbar$ -curve for the function *g*.

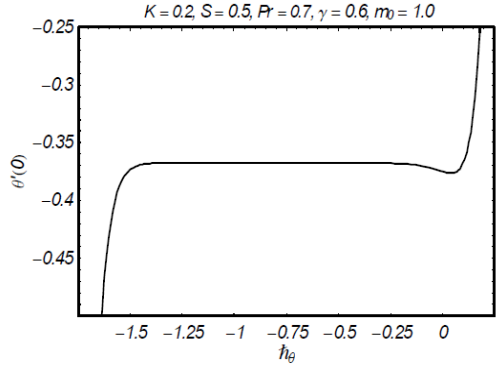

Fig. 3. $\hbar$ -curve for the function θ.

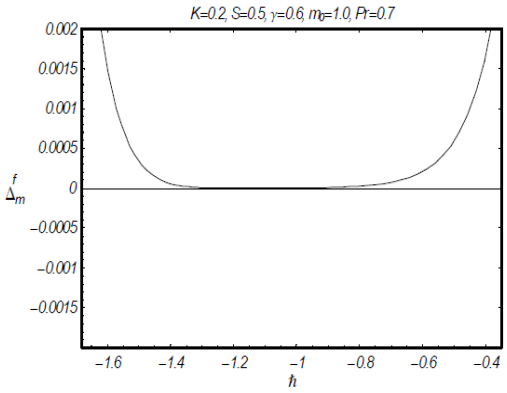

Fig. 4(a). $\hbar$ -curve for the residual error Δ_m^f.

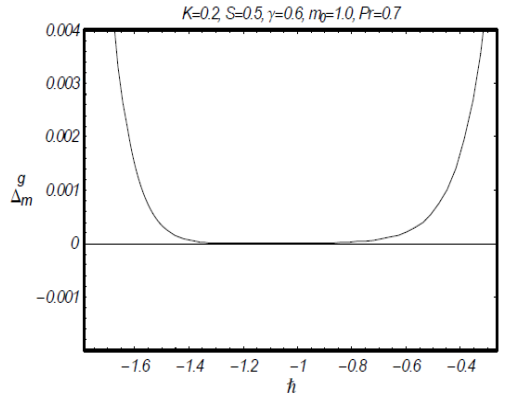

Fig. 4(b). $\hbar$ -curve for the residual error Δ_m^g.

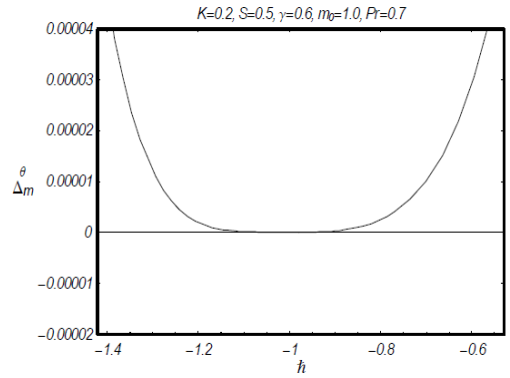

Fig. 4(c). $\hbar$ -curve for the residual error Δ_m^θ.

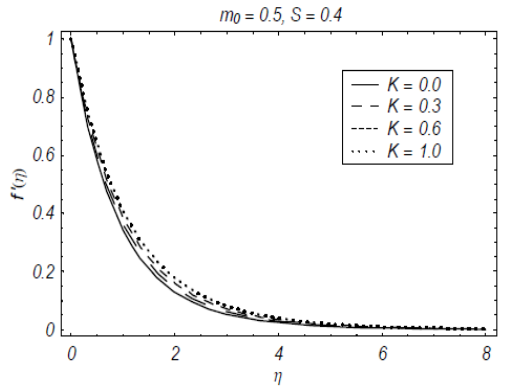

Fig. 5. Effects of *K* on f'.

Table 1 Convergence of homotopy solution for different order of approximations when $K = 0.2$, $S = 0.5$, $\gamma = 0.6$, $\Pr = 0.7$, $m_0 = 1$ **and** $\hbar_f = \hbar_g = \hbar_\theta = -0.7$

Order of approximations	$-f''(0)$	$-g'(0)$	$-\theta'(0)$
1	1.13125	0.38500	0.37315
5	1.16799	0.51648	0.36819
10	1.16798	0.51697	0.36761
15	1.16798	0.51697	0.36754
20	1.16798	0.51697	0.36754
25	1.16798	0.51697	0.36754
30	1.16798	0.51697	0.36754
40	1.16798	0.51697	0.36754

4. DISCUSSION

This section aims to study the influence of physical parameters on the velocity, micro-rotation velocity and the temperature fields. This objective is achieved through plots of Figs. 5-14 for the effects of micropolar parameter K, unsteadiness parameter S, boundary parameter m_0, Prandtl number Pr and Biot number γ on the velocity component f', the micro-rotation velocity g and the temperature profile θ respectively. Further, numerical values of the skin-friction coefficient and the local Nusselt number are computed in the Tables 2 and 3. Figs. 5-14 address the variations of micropolar parameter K, unsteadiness parameter S and boundary parameter m_0 on the velocity field f'. Here Fig. 5 shows the effects of micropolar parameter K on the velocity f'. This Fig. shows that f' is an increasing function of K. The boundary layer thickness increases when K increases. The material parameter give rise to the fluid flow and an increase in the velocity and momentum boundary layer thickness is observed. Physically an increase in micropolar parameter leads to a decrease in the dynamic viscosity. This decrease in the dynamic viscosity is responsible for the enhancement in the fluid velocity. A decrease in the dynamic viscosity implies to the less viscous fluid. The less viscous fluid has higher velocity due to less resistance to flow. Fig. 6 shows the variations of unsteadiness parameter S on f'. Here the velocity f' is found to decrease when S increases. The boundary layer thickness also decreases when S is increased. We observed that the unsteadiness parameter resists the fluid flow which yields a decrease in the velocity. Fig. 7 depicts the influence of boundary parameter m_0 on f'. The boundary parameter reduced the velocity and momentum boundary layer thickness.

Figs. 8-10 are plotted for the variations of K, S and m_0 on the microrotation velocity profile g. Fig. 8 presents the influence of K on g. It is observed that initially g decreases by increasing K. It can also be seen from this Fig. that the micro rotation velocity g is greater when compared with Newtonian case ($K = 0$) for large values of K. The boundary layer thickness also decreases as K increases. Fig. 9 depicts the effects of S on g. Initially g increases when S increases but when we move away from the surface then both g and boundary layer decrease. Fig. 10 depicts the effects of boundary parameter m_0 on micro-rotation velocity g. The micro-rotation velocity g is an increasing function of m_0. The boundary layer thickness is increased for large values of m_0. The micro-rotation velocity is increasing rapidly by increasing the values of boundary parameter m_0. It is also observed that for $m_0 = 0$, the micro-rotation velocity is zero.

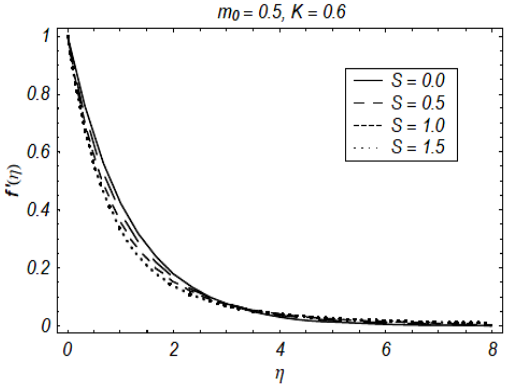

Fig. 6. Effects of *S* on f'.

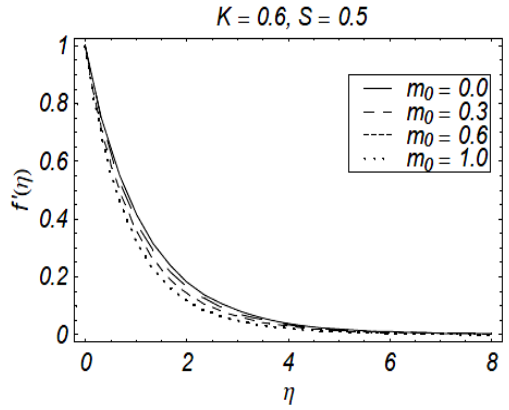

Fig. 7. Effects of m_0 on f'.

Figs. 11-14 illustrate the effects of S, m_0, Pr and γ on the temperature profile θ. Fig. 11 shows the variation of S on θ. It is noted that temperature profile θ decreases when S increases. The thermal boundary layer thickness also decreases for large values of S. An increase in unsteadiness parameter reduces the heat of fluid that leads to a decrease in the temperature and its related boundary layer thickness. Temperature is higher for smaller values of unsteadiness parameter and lower for larger values of unsteadiness parameter. Fig. 12 illustrates the effects of boundary parameter m_0 on

temperature profile θ. From this Fig. one can see that the temperature profile and thermal boundary layer thickness increase when m_0 is increased. Influence of Pr on θ can be seen in Fig. 13. From the definition of Prandtl number, it is seen that an increase in Prandtl number corresponds to a smaller thermal diffusivity. Due to smaller thermal diffusivity, a reduction in temperature and thermal boundary layer thickness appears. In fact fluids with smaller Prandtl number have higher thermal diffusivity and larger Prandtl fluids have lower thermal diffusivity. In industry, Prandtl number is used to control the cooling rate during the manufacture process. Fig. 14 shows the effects of γ on θ. It is evident from this Fig. that when γ increases temperature profile θ as well as thermal boundary layer thickness increase. In fact the Biot number involves the heat transfer coefficient. The heat transfer coefficient increases with an increase in Biot number. An increase in heat transfer coefficient give rise to the temperature and thermal boundary layer thickness. Here we have seen that for $\gamma = 0$, there is no heat transfer at the wall. Further we examined that the temperature at the wall is increased suddenly for $\gamma = 0.5$ but for $\gamma = 1.0$ and 1.5, such increase in temperature is very slow.

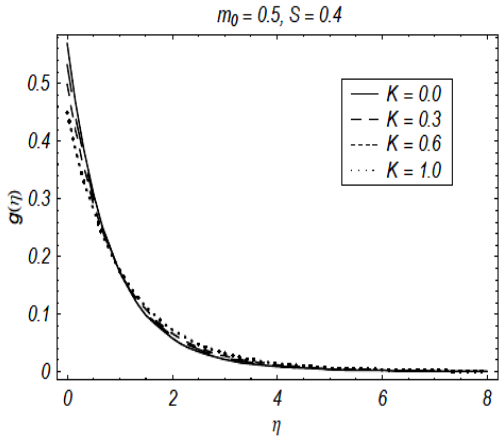

Fig. 8. Effects of *K* on *g*.

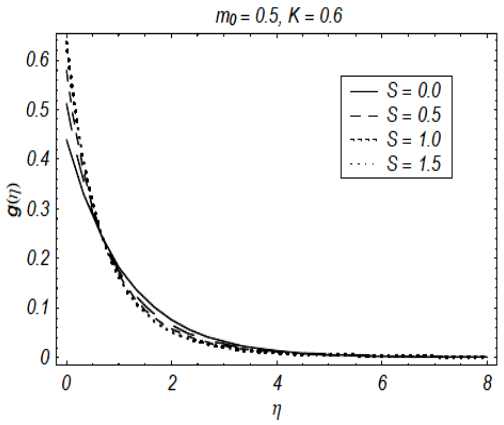

Fig. 9. Effects of *S* on *g*.

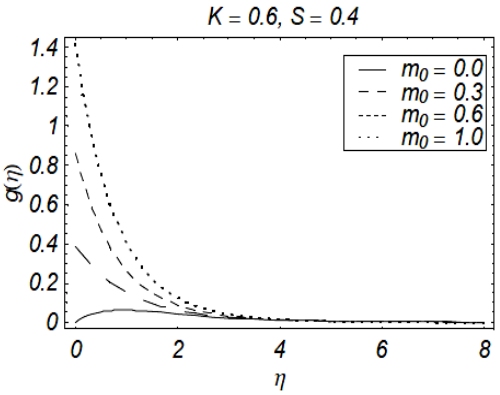

Fig. 10. Effects of m_0 on *g*.

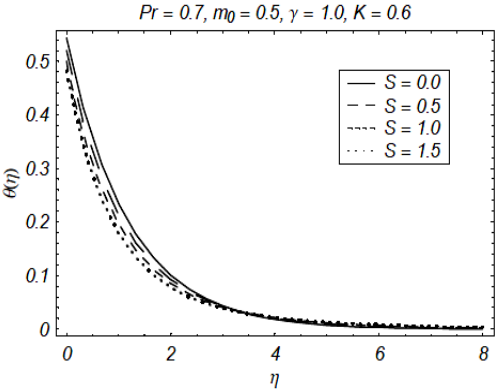

Fig. 11. Effects of *S* on θ.

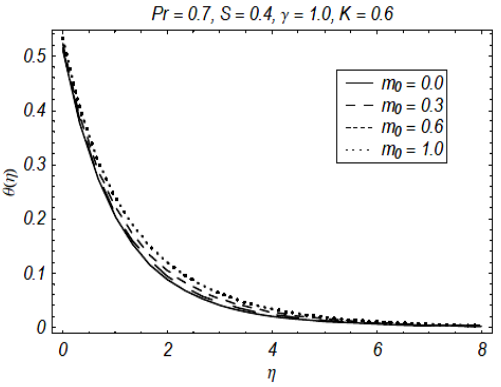

Fig. 12. Effects of m_0 on θ.

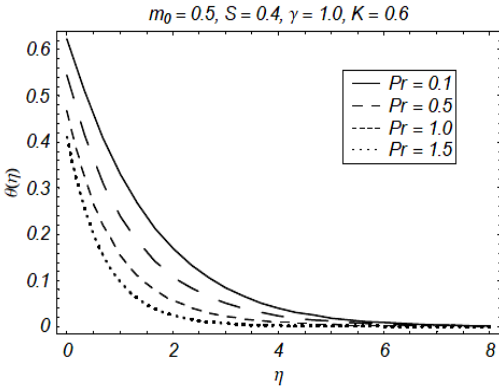

Fig. 13. Effects of *Pr* on θ.

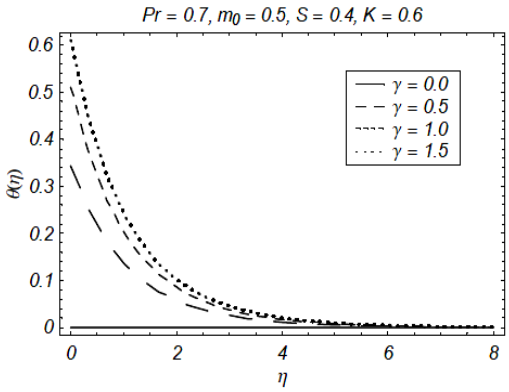

Fig. 14. Effects of γ on θ.

Table 2 Numerical values of skin friction coefficient $Cf_x \mathrm{Re}_x^{1/2}$ for various values K, S and m_0.

K	S	$m_0 = 0.0$	$m_0 = 0.5$	$m_0 = 1.0$
$Cf_x \mathrm{Re}_x^{1/2}$				
0.1	0.5	-1.2233	-1.1961	-1.1674
0.3		-1.3240	-1.2517	-1.1688
0.5		-1.4135	-1.3050	-1.1706
0.4	0.0	-1.1713	-1.0954	-1.0051
	0.3	-1.2920	-1.2069	-1.1052
	0.5	-1.4079	-1.3136	-1.2010

To see the convergent values of $-f''(0)$, $-g'(0)$ and $-\theta'(0)$ for the fixed values of emerging parameters, Table 1 is computed. This Table shows that series solutions for velocity and micro rotation converge from 10th order of approximations and for temperature it converges from 15th order of deformations. Also we observed that the values of $-f''(0)$ are higher in comparison to the values of $-g'(0)$ and $-\theta'(0)$. Tables 2 and 3 show the numerical values of skin-friction coefficient and local Nusselt number. From Table 2, it is noted that the magnitude of skin-friction coefficient increases for large values of K and S but it decreases for the larger values of m_0. The values of skin-friction coefficient are larger for smaller values of boundary parameter. It is also examined from this Table that all the values of skin-friction coefficient are negative. This negative sign is due to the drag force that surface exerts on the fluid. From Table 3, the values of heat transfer rate become large when we increase the values of γ, K, Pr and S. However the heat transfer rate becomes smaller with an increase in m_0. The reduction in the values of local Nusselt number is very small by increasing m_0.

5. CONCLUSIONS

We have studied the time-dependent boundary layer flow of micropolar fluid with heat transfer. Heat transfer is characterized due to convective surface condition. The flow is caused due to the unsteady stretching surface. The main results are listed below:

- Velocity f' is decreasing function of S and m_0.
- Both temperature and thermal boundary layer thickness are decreased when Pr increases.
- Behavior of m_0 and Pr on the temperature are quite opposite.
- Microrotation profile decreases when m_0 is increased.
- The values of skin-friction coefficient are reduced with the increasing values of boundary parameter.
- Values of local Nusselt number increase when γ and K are increased.

Table 3 Numerical values of Local Nusselt number $-\theta'(0)$ for various values K, S, m_0, Pr, and γ.

γ	K	m_0	Pr	S	$-\theta'(0)$
0.3	1.0	0.5	1.0	0.7	0.24235
0.5					0.35805
0.7					0.45015
0.9					0.52521
0.6	0.0				0.37935
	0.3				0.38062
	0.6				0.38169
	0.9				0.38261
	0.4	0.0			0.38232
		0.2			0.38182
		0.4			0.38128
		0.6			0.38069
		0.5	0.4		0.33757
			0.8		0.39311
			1.2		0.42239
			1.5		0.43729
			1.0	0.0	0.38161
				0.5	0.40018
				1.0	0.41514
				1.5	0.42720

REFERENCES

Abbasbandy, S. and E. Shivanian (2011). Predictor homotopy analysis method and its application to some nonlinear problems, *Commun. Nonlinear Sci. Numer. Simulat.* 16, 2456-2468.

Andersson, H. I., J. B. Aarseth and B. S. Dandapat (2000). Heat transfer in a liquid film on an unsteady stretching surface, *Int. J. Heat Mass Transfer* 43, 69-74.

Bachok, N., A. Ishak and R. Nazar (2011). Flow and heat transfer over an unsteady stretching sheet in a micropolar fluid, *Meccanica* 46, 935-942.

Devi, C. D. S., H. S. Takhar and G. Nath, (1991). Unsteady mixed convection flow in stagnation region adjacent to a vertical surface, *Heat Mass Transfer* 26, 71-79.

Eringen, A. C. (1966). Theory of micropolar fluids,

J. Math. Mech. 16, 1-18.

Eringen, A. C. Theory of thermomicro fluids, *J. Math. Anal. Appl.*, 38, 480-496.

Hayat, T., M. Farooq, Z. Iqbal and A. Alsaedi (2012). Mixed convection Falkner-Skan flow of a Maxwell fluid, *J. Heat Transfer-Transactions ASME* 134, 114504.

Hayat, T., S. A. Shehzad and A. Alsaedi, (2012). Soret and Dufour effects on magnetohydrodynamic (MHD) flow of Casson fluid, *Appl. Math. Mech. Eng. Edit.* 33, 1301-1312.

Hayat, T., S. A. Shehzad and M. Qasim (2011). Mixed convection flow of a micropolar fluid with radiation and chemical reaction, *Int. J. Numer. Meth. Fluids* 67, 1418-1436.

Hayat, T., S. A. Shehzad, A. Alsaedi and M. S. Alhothuali (2012). Mixed convection stagnation point flow of Casson fluid with convective boundary conditions, *Chin. Phys. Lett.* 29, 114704.

Hayat, T., S. A. Shehzad, A. Rafique and M. Y. Malik, (2012). Mixed convection unsteady stagnation point flow over a stretching sheet with heat transfer in the presence of variable free stream, *Int. J. Numer. Methods Fluids* 88, 483-493.

Hayat, T., S. A. Shehzad, M. Qasim and S. Obaidat, (2011). Flow of second grade fluid with convective boundary conditions, *Thermal Sci.* 15, S253-S261.

Hayat, T., Z. Abbas and T. Javed (2008). Mixed convection flow of a micropolar fluid over a non-linearly stretching sheet, *Phys. Lett. A* 372, 637-647.

Ishak, A., L. Y. Yian and I. Pop (2010). Stagnation point flow over a shrinking sheet in a micropolar fluid, *Chem. Eng. Commun.* 197, 1417-1427.

Ishak, A., R. Nazar and I. Pop (2008). Heat transfer over a stretching surface with variable heat flux in micropolar fluids, *Phys. Lett. A* 372, 559-561.

Ishak, A., R. Nazar and I. Pop (2008). Stagnation flow of a micropolar fluid towards a vertical permeable surface, *Int. Commun. Heat Mass Transfer* 35, 276-281.

Ishak, A., R. Nazar and I. Pop (2009). Heat transfer over an unsteady stretching permeable surface with prescribed wall temperature, *Nonlinear Anal.-Real World Appl.* 10, 2909-2913.

Liao, S. J. (2003). Beyond Perturbation: Introduction to Homotopy Analysis Method, Chapman & Hall/CRC Press, Boca Raton.

Makinde, O. D. (2010). On MHD heat and mass transfer over a moving vertical plate with a convective surface boundary condition, *Canadian J. Chem. Eng.* 88, 983-990.

Makinde, O. D. (2012). Computational modelling of MHD unsteady flow and heat transfer toward a flat plate with Navier slip and Newtonian heating, *Braz. J. Chem. Eng.* 29, 159-166.

Makinde, O. D. and A. Aziz (2010). MHD mixed convection from a vertical plate embedded in a porous medium with convective boundary condition, *Int. J. Thermal Sci.* 49, 1813-1820.

Motsa, S. S., S. Shateyi and P. Sibanda (2010). A model of steady viscous flow of a micropolar fluid driven by injection or suction between a porous disk and a non-porous disk using a novel numerical technique, *Canadian J. Chem. Eng.* 88, 991-1002.

Nazar, R., N. Amin and I. Pop (2004). Unsteady boundary layer flow due to stretching surface in a rotating fluid, *Mech. Res. Commun.* 31, 121-128.

Nazar, R., N. Amin, D. Filip and I. Pop (2004). Stagnation point flow of a micropolar fluid towards a stretching sheet, *Int. J. Non-Lin. Mec.* 39, 1227-1235.

Peddieson, J. and R. P. McNitt (1970). Boundary-layer theory for a micropolar fluid, *Recent Adv. Eng. Sci.* 5, 405-426.

Rashidi, M. M. and E. Erfani (2012). Analytical method for solving steady MHD convective and slip flow due to a rotating disk with viscous dissipation and Ohmic heating. *Eng. Computations* 29, 562-579.

Rashidi, M. M., E. Momoniat and B. Rostami, (2012). Analytic approximate solutions for MHD boundary-layer viscoelastic fluid flow over continuously moving stretching surface by homotopy analysis method with two auxiliary parameters, *J. Appl. Math.* 780415.

Rashidi, M. M., S. A. M. Pour and N. Laraqi (2010). A semi-analytical solution of micropolar flow in a porous channel with mass injection by using differential transform method, *Nonlinear Analysis: Modelling and Control* 15, 341-350

Sajid, M., Z. Abbas and T. Hayat (2009). Homotopy analysis for boundary layer flow of a micropolar fluid through a porous channel, *Appl. Math. Modelling* 33, 4120-4125.

Shehzad, S. A., F. E. Alsaadi, S. J. Monaquel and T. Hayat (2013). Soret and Dufour effects on the stagnation point flow of Jeffery fluid with convective boundary conditions, *Europ. Phys. J. Plus* 128, 56.

Shehzad, S. A., M. Qasim, A. Alsaedi, T. Hayat and M. S. Alhuthali (2013). Combined effects of thermal stratification and thermal radiation in mixed convection flow of thixotropic fluid, *Europ. Phys. J. Plus* 128, 7.

Shehzad, S. A., M. Qasim, T. Hayat, M. Sajid and S. Obaidat (2013). Boundary layer flow of Maxwell fluid with power law heat flux and

heat source, *Int. J. Numer. Methods Heat Fluid Flow* 23, 1225-1241.

Shehzad, S. A., T. Hayat, S. Asghar and A. Alsaedi (2015). Stagnation point flow of thixotropic fluid over a stretching sheet with mass transfer and chemical reaction, *J. Appl. Fluid Mech.* 8, 465-471.

Yacob, N. A. and A. Ishak (2012). Micropolar fluid flow over a shrinking sheet, *Meccanica* 47, 293-299.

Yacob, N. A., A. Ishak and I. Pop (2011). Melting heat transfer in boundary layer stagnation-point flow towards a stretching/shrinking sheet in a micropolar fluid, *Comput. Fluids* 47, 16-21.